ATLANTIS PRESS

Atlantis Highlights in Engineering, volume 4

13th International Renewable Energy Storage Conference (IRES 2019)

Power Quality in Smart Distribution Systems with Electric Battery, Large Loads and PV Generation.

1st Miguel Muñoz Ortiz
Operations Research and Economics
Sintef AS
Trondheim, Norway
miguel.ortiz@sintef.no

2nd Idar Petersen
Active Power Networks
Sintef Energi AS
Trondheim, Norway
idar.petersen@sintef.no

3rd Ralf Mikut
Institute for Automation and Applied Informatics
Karlsruhe Institute of Technology
Karlsruhe, Germany
ralf.mikut@kit.edu

4th Henrik Landsverk
Research and Development
Skagerak Nett AS
Porsgrunn, Norway
henrik.landsverk@skagerakenergi.no

5th Stig Harald Simonsen
Research and Development
Skagerak Nett AS
Porsgrunn, Norway
stig.simonsen@skagerakenergi.no

***Abstract*—A change in the electricity consumption is taking place, where one of the main reasons is the large increase in Distributed Generation, as photovoltaic (PV) systems and electric batteries in the low voltage (LV) distribution grid. This could translate in specific cases into a situation of increased peak load and bigger voltage fluctuation. Therefore, an effective control of the grid voltage is necessary to achieve a stable energy supply from renewable sources. What services can a battery provide? The authors present an analysis of voltage control and other battery services in a LV grid. A flexible model based on Python is developed and used to solve a multi-period optimal power flow problem. They propose an optimised distributed voltage regulation. The power flow equations are linearised around a stable operation point, which allows high feasibility and computation speed. Then a receding horizon framework is described, including 24h and 1h updated forecasts. The analysis is performed on a LV network with large loads of a stadium, large PV generation (690kWp) and with a 1MWh battery. The new method provides an optimization of the grid operation (reduced voltage variation and cost of energy imported from the grid) under different seasonal weeks.**

***Index Terms*—Battery use, voltage control, complex power, multi-period optimal power flow, receding horizon, low voltage, PV**

I. Introduction

Energy plays a critical role in today's society. Human beings rely on technology in most parts of the world, which depends heavily on energy availability. Traditional energy sources are fossil-based (e.g. coal, petroleum, natural gas), which inherently translate into pollution of the environment, climate change and limited supply [1]. These limitations have conducted scientists, industry and society to develop and use other types of energy sources which are more environmentally friendly and which do not have limited availability. Moreover, different international and national agreements seek to set limits to harmful gas emissions and increase the share of renewable energy generation. For example, Germany's Energiewende plans to increase above 50 % of renewable energy share by 2050 [2] in Germany.

A consequence of renewable energy sources is the popularisation of decentralised energy generation, where energy is produced in small locations instead of big power plants. This, added to the fluctuation and the uncertainty of many of the renewable energy sources used (e.g. wind, PV) puts attention to the operation of distribution networks by using new technologies to control the parameters that guarantee an efficient and stable electricity distribution [3]. The current grid was designed for the past energy situation, where big power plants produced large amounts of energy which is then distributed to the consumers, and the technologies for control, measurement and communication were not well developed. Nowadays, the ability to easily measuring parameters in the grid and the largest presence of distributed energy generation allows a wider use of different electricity tariffs and other business models. Examples of these business models include self-sufficiency of consumers with own generation or even selling the excessive energy, also called prosumers. Thus, the future grid will become more complex and challenging to manage [4]. The presence of renewable generation such as PV and wind increase uncertainty in energy production. To tackle this problem several studies address different ways to consider uncertainty in energy dispatchers, by combining uncertainty of PV generation and load as in [5], and extending it to include electric vehicle state of charge uncertainty in [6]. That causes the sampling period to be reduced from hours to minutes [7]. Nowadays with the help of smart meters, the ability to read loads and generation values from 1 minute to two hours allows better control over the LV distribution network [8]. In literature it is common to see analysis performed on data with 15 minute resolution [9], [10]. Nevertheless, this work is more oriented to 15 minute resolution schedules (though available

data has hourly resolution) and not very-short time voltage stabilization.

One of the most noticeable changes occurring in the distribution networks is the significant increase in the share of distributed generators (DG), such as PV solar power integration [11]. The inverter systems (for PV or battery) can provide reactive power control [12], which can help to regulate distribution network voltages. In cases where loads are large and there is a deficit of reactive power support, the voltage stability might be at risk. With the increasing amount of installed DG, a study of voltage in the distribution network might be necessary [11].

Several contributions in literature address the optimal voltage control of distribution networks with large amount of DG, such as high presence of PV and batteries. There are different approaches in the literature to this topic. Some authors [13] focus on analysing a distribution network with PV generation and a battery, employing linearised AC Power Flow Equations, addressing PV uncertainty and including a battery model. However, the combined study of big centralised battery uses (especially for voltage control) and the economic study in LV grids is not easily found in literature. In [14], some different grid services that a battery can provide are analysed, giving promising results for battery presence in the distribution grid. On the other hand, voltage control is left for future work. The studies done in [15], [16] show that a big centralised battery is more appropriate for a grid with voltage deviation, to achieve lower distribution losses and to mitigate thermal overload of distributed generation at LV levels. There are some works that analyse the coordination between PV and On-Load Tap Changer and PV inverters [17], but where battery is not considered.

An extensive study of the value of battery has been done in [18]. There, the different services that a battery can provide and the added value are thoroughly explained. Nevertheless, in the case of voltage regulation there is only one study to be found, and for other services its value depends greatly on the project. Therefore, more study cases are relevant to acquire new knowledge about the value of batteries. Another real case study of battery uses is done in [14], but leaves voltage control provided by the battery for future work. Different studies that treat different battery uses for grid applications include [19] and [20]. Their conclusions contribute positively for battery installation in grids, and specifically in LV networks, though they mention the need for more models and validation of them using real data. This paper analyses the influence of a big battery and PV located in a LV network, as opposed to the common decentralised PV and battery systems analysed in literature.

The greater part of battery studies and renewable penetration is done in medium voltage (MV) networks [21], [22], and there are not many open data sets available for European LV standard distribution feeders. IEEE Power and Energy society has only recently developed standard LV networks [23], and another smaller LV options are described in [24].

Nonetheless, there is a good contribution to battery usage and LV Optimal Power Flow in [25], [26], [27]. The main focus is set on battery siting and sizing and developing different methods to obtain accurate, but computationally inexpensive formulations for the Power Flow Equations. This topic is out of the scope of this paper, which on the other hand, uses a linearisation of the equations around the operating point.

In [28], a receding horizon control algorithm has been proposed with the objectives of minimising line losses and storage use in a real LV network. However, the different uses of the batteries are not analysed. A voltage control analysis is performed in [29], but considers that PV and battery are connected to the same bus being the main focus voltage control through the PV inverter.

In this paper, an optimised distributed voltage regulation scheme is proposed that uses the inverters of batteries and PV, as well as the battery capacity to control the voltage and to provide other services. Additionally, a novel tool for distribution grid voltage control optimisation is developed considering uncertainty in PV generation in a receding horizon with low computational effort. This tool is employed on a real demo-case based on a football stadium. The objective is to study the cost-benefit on improved voltage regulation and other uses of the battery.

This paper summarises the most important aspects developed in the master's thesis [30]. This thesis is part of the IntegER[1] project, which is an Innovation Project in Business and Industry (IPN), with founding from the Research Council of Norway under the ENERGIX[2] programme. The project aims to find new guidelines and acquire knowledge for the use of storage (mainly batteries) and its integration into the Norwegian distribution grid. Therefore, the role of the battery and its possible uses is studied in detail.

As part of the development of the ideas of this paper, a demo-case is analysed. Skagerak EnergiLAB[3] serves as an example of a distribution grid, with a large penetration of PV contribution ($5330m^2$ installed on the roof of the stadium, 3230 PV modules with $690kWp$ installed capacity) and as well as the presence of a battery with $1MWh/1MW$ capacity, both connected to a different substation in the grid. The current topology looks this way because the main stadium loads and PV are connected to a substation and the battery, floodlights and other loads are connected to a second substation. However, one of the topologies of interest is a microgrid connecting both substations including PV and battery in the same network. The schematics of the network are displayed in Figure 1.

Regarding tools available to solve optimal power flow problems, some MATLAB-based tools exist, like MATPOWER [31], as well as Python-based toolboxes [32]. However, as

[1]Link to the project: https://www.sintef.no/en/projects/integer-integration-of-energy-storage-in-the-distribution-grid/

[2]Link to the programme: https://www.forskningsradet.no/prognett-energix/

[3]Link (Norwegian): https://www.skageraknett.no/skagerak-energilab/category1560.html

part of IntegER project, an in-house flexible tool to study electric storage was desired. The new tool allows the study of different electric power systems where battery and distributed generation are present.

This paper is structured as follows. In Section II the problem formulation is described. The demo-case is presented in Section III. The receding horizon algorithm used in the simulation is shown in Section IV. Finally, the results of the simulations are explained in Section V and Section VI presents the conclusions and future work.

II. Problem Formulation

In this section, the theoretical and mathematical formulation of the demo-case $N = 30$ bus system is modelled with power-based considerations, for the required voltage control analysis. It is modelled as a single line network and referenced to a per unit system to handle the different voltages. The general assumptions taken in this paper are:

- The slack bus can provide the required active and reactive power.
- A linearisation of the power flow equations is described in this section. This results in simplification and fast solving of the problem.
- The LV distribution network is considered as a single-line AC grid. The lines are considered short, so that no shunt admittance is present.
- PV system and battery are modelled through the complex power provided or absorbed by the inverter, considering that the AC active power is equal to the DC power of these systems.

A bus set $Set_{bus} = [1, ..., N]$ is defined with the number of buses of the system. The slack bus is set to bus number 1. The system has a battery connected in bus $n_B \in Set_{bus}$ and a PV system connected to a different bus $n_{pv} \in Set_{bus}$, where $n_B \neq n_{pv} \neq 1$. The model is done using Python[4] (version 3.6) and one of its optimisation packages (Pyomo, [33]). The system changes over time in the time period $t \in [1, ..., T]$, where T is the simulation horizon. The model of the different distribution network units is done similarly to the one suggested by [34], which collects common practices and assumptions used in literature for Optimal Power Flow problems in distribution grids.

A. Modelling the Line Limits

A way to model line limitations is by setting a constraint that limits the current flowing through each line.

$$-I_{lim} \leq \sum_{j=1}^{N} (V_i(t) - V_j(t)) \cdot Y_{ij} \leq I_{lim} \quad \forall i \in Set_{bus} \quad (1)$$

[4]https://www.python.org/

B. Slack Bus

The slack bus is defined in this system as bus 1, where power is exchanged with the grid (exporting and importing). P_1 is the net power in bus 1 and if P_1 is positive, the system imports energy from the grid and if negative the system exports energy to the grid. Reactive power (Q_1) is also provided by the slack bus when it is required by the system. The maximum active and reactive power exchanged is limited at the bus 1.

$$P_{\min} \leq P_1(t) \leq P_{\max} \quad (2)$$

$$Q_{\min} \leq Q_1(t) \leq Q_{\max} \quad (3)$$

To determine how much power is exported and imported, two positive variables are defined: P_{export} and P_{import}.

$$P_1(t) = P_{import}(t) - P_{export}(t) \quad (4)$$

$$P_{export}(t) \geq 0, \quad P_{import}(t) \geq 0 \quad (5)$$

C. General Bus with Generation and Load

The rest of buses $i \neq 1$ are PQ buses with generation and load is composed with an active, P_i^G and P_i^L and reactive component, Q_i^G and Q_i^L, where G represents the generation power and L the load. In case that no load or generation is present at a specific bus, values are equal to 0.

$$P_i(t) = P_i^G(t) - P_i^L(t) \quad (6)$$

$$Q_i(t) = Q_i^G(t) - Q_i^L(t) \quad (7)$$

D. PV Modelling

The PV system is capable of providing reactive power using an inverter. The total apparent power that the inverter is capable to inject to the grid is defined as $S_{inv,n_{pv}}$, and the generation power of the PV system ($P_{n_{pv}}^G$ and $Q_{n_{pv}}^G$) is limited by the apparent power, as seen in equation (8).

$$S_{inv,n_{pv}}^2(t) \geq (P_{n_{pv}}^G)^2(t) + (Q_{n_{pv}}^G)^2(t) \quad (8)$$

The active power generated by the PV system is assumed to be equal to the maximum power point, $P_{MPPT,n_{pv}}$ produced by the PV model.

$$P_{n_{pv}}^G(t) = P_{MPPT,n_{pv}}(t) \quad (9)$$

In order to limit the reactive power that can be used, it is controlled by the limitations of the inverter, as shown in equation (10).

$$Q_{inv,n_{pv},\min} \leq Q_{n_{pv}}^G \leq Q_{inv,n_{pv},\max} \quad (10)$$

A bus n_{PV} is composed by a PV system that works as a generator and a load in that bus.

$$P_{n_{pv}}(t) = P_{n_{pv}}^G(t) - P_{n_{pv}}^L(t) \quad (11)$$

$$Q_{n_{pv}}(t) = Q_{n_{pv}}^G(t) - Q_{n_{pv}}^L(t) \quad (12)$$

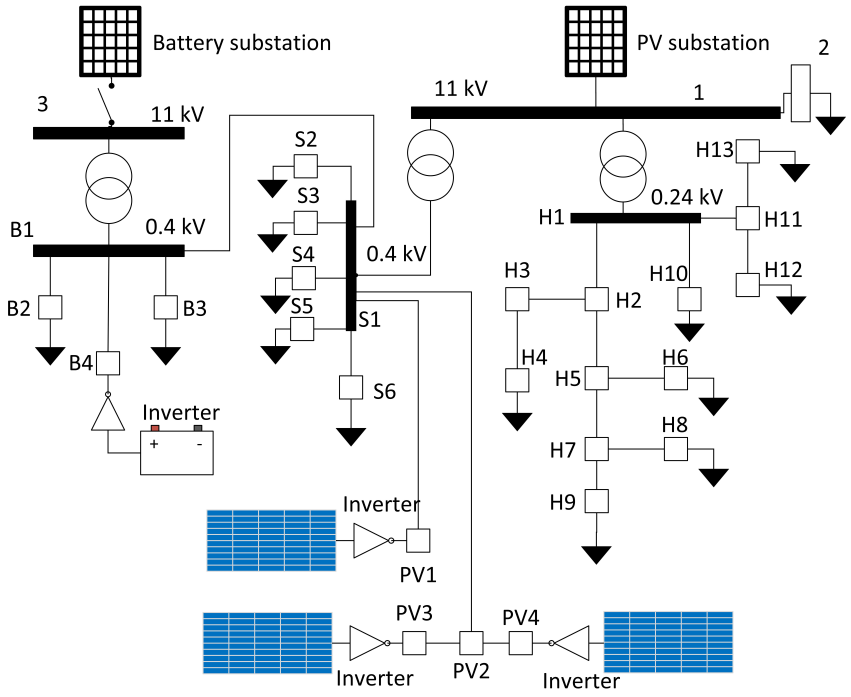

Fig. 1. The topology of the demo-case. Bars represent bus bars at different voltages, two circles interconnected represent transformers between the networks with different nominal voltage, squares and rectangles represent nodes, black arrows loads, triangles are inverters (battery and PV). The blue squares represent PV modules and the battery is indicated as a battery symbol. Nodes are connected through lines. Each node is defined by a name composed of a number (e.g. 1), which are the medium voltage nodes or a combination of letters and a number (e.g. $B1$ or $S2$) which are the nodes at low voltage, defining the letter the subnetwork where the node is located: B is the battery subnetwork, S the main stadium subnetwork, PV is the PV system and H the household and commercial subnetwork.

E. Battery Modelling

The battery is modelled using the equations eqs. (13) to (17) described below. SoC describes the state of charge of the battery and η_{ch} and η_{disch} are the efficiencies of charge and discharge respectively. The charge and discharge power, which are positive are defined as P_{ch} and P_{disch} respectively, with Δt as the length of each time step.

$$SoC(t) = SoC(t-1) - P_{disch}(t)\cdot\Delta t\cdot\frac{1}{\eta_{disch}} + P_{ch}(t)\cdot\Delta t\cdot\eta_{ch} \tag{13}$$

$$SoC(t) \leq SoC_{\max} \tag{14}$$

$$SoC(t) \geq SoC_{\min} \tag{15}$$

$$0 \leq P_{ch}(t) \leq P^{ch}_{\max} \tag{16}$$

$$0 \leq P_{disch}(t) \leq P^{disch}_{\max} \tag{17}$$

F. Bus with Battery and Load

The battery is located at bus n_B and it behaves both as a load (when charging the battery) and as a generator (when discharging), and the battery inverter can absorb and inject reactive power to the grid, defined as Q_{abs} and Q_{inj}. Thus, the generation and load power at the bus is described in equations eqs. (18) to (21).

$$P^G_{n_B}(t) = P_{disch}(t) - P_{ch}(t) \tag{18}$$

$$P^L_{n_B}(t) = P^{load}_{n_B} \tag{19}$$

$$Q^G_{n_B}(t) = Q_{inj}(t) - Q_{abs}(t) \tag{20}$$

$$Q^L_{n_B}(t) = Q^{load}_{n_B}(t) \tag{21}$$

The power balance at the bus is then defined in equations (22) and (23).

$$P_{n_B}(t) = P^G_{n_B}(t) - P^L_{n_B}(t) \tag{22}$$

$$Q_{n_B}(t) = Q^G_{n_B}(t) - Q^L_{n_B}(t) \tag{23}$$

The total power at the bus has to fulfil the limitations of the inverter.

$$S^2_{inv,n_B}(t) \geq (P_{disch}(t) - P_{ch}(t))^2 + (Q_{inj}(t) - Q_{abs}(t))^2 \tag{24}$$

The reactive power injected and absorbed can be limited.

$$Q_{inv,n_B,\min} \leq (Q_{inj}(t) - Q_{abs}(t)) \leq Q_{inv,n_B,\max}, \quad Q_{inj}(t) \geq 0, \quad Q_{abs}(t) \geq 0 \tag{25}$$

G. Power Flow

The classical power flow equations for each node i over the rest of the nodes j are written below.

$$P_i(t) = \sum_{j=1}^{N} Y_{ij}[V_i(t)\cdot V_j(t)\cdot\cos(\delta_i(t))\cdot\cos(\delta_i(t)+\theta_{ij}) + V_i(t)\cdot V_j(t)\cdot\sin(\delta_i(t))\cdot\sin(\delta_i(t)+\theta_{ij})] \tag{26}$$

$$Q_i(t) = \sum_{j=1}^{N} Y_{ij}[V_i(t) \cdot V_j(t) \cdot \sin(\delta_i(t)) \cdot \cos(\delta_i(t) + \theta_{ij}) - V_i(t) \cdot V_j(t) \cdot \cos(\delta_i(t)) \cdot \sin(\delta_i(t) + \theta_{ij})] \quad (27)$$

The equations are subject to voltage limitations.

$$V_{\min} \leq V_i(t) \leq V_{\max} \ \forall i \in Set_{bus} \quad (28)$$

The Power Flow Equations are non-linear and computationally demanding to solve. Therefore, simplifications are commonly found in literature [26]. One of the possible solutions is to linearise the equations around an operation point, which is achieved by means of first order Taylor series. A similar approach is done in [35]. This simplifies the cost sacrificing accuracy, but considering the complexity of power flow equations and the scope of the paper this is a reasonable assumption. The mathematical expression of the n order Taylor series can be seen in equation (29).

$$F(x) = \sum_{n=0}^{\infty} \frac{f^{(n)}(x_0)}{n!} \cdot (x - x_0) \quad (29)$$

Where,

$F(x)$: The linear version of the original function

f : The function to be linearised

n : The order of the derivative

x : The variable of the function f

x_0 : The operational point of the linearisation

By rearranging the equations (26) and (27), grouping sets of variables, they can be expressed as in (30) and (31).

$$P_i(t) = \sum_{j=1}^{N} Y_{ij}[f_{ijA}(t) + f_{ijB}(t)] \quad (30)$$

$$Q_i(t) = \sum_{j=1}^{N} Y_{ij}[g_{ijA}(t) + g_{ijB}(t)] \quad (31)$$

Where,

$$f_{ijA}(t) = V_i(t) \cdot V_j(t) \cdot \cos(\delta_i(t)) \cdot \cos(\delta_i(t) + \theta_{ij})$$
$$f_{ijB}(t) = V_i(t) \cdot V_j(t) \cdot \sin(\delta_i(t)) \cdot \sin(\delta_i(t) + \theta_{ij})$$
$$g_{ijA}(t) = V_i(t) \cdot V_j(t) \cdot \sin(\delta_i(t)) \cdot \cos(\delta_i(t) + \theta_{ij})$$
$$g_{ijB}(t) = -V_i(t) \cdot V_j(t) \cdot \cos(\delta_i(t)) \cdot \sin(\delta_i(t) + \theta_{ij})$$

The main aspect of the linearisation process is to evaluate f_{1i}, f_{2i}, g_{1i} and g_{2i} around the working point x_0, represented by the following per unit values,

$$(V_{i0}, V_{j0}, \delta_{i0}, \delta_{j0}) = (1, 1, 0, 0)$$

When the proposed linearisation method is applied, each linear equation can be named h_m and its linearisation is solved as follows,

$$h_m = h(V_i, V_j, \delta_i, \delta_j)$$

$$h_{m0} = h(V_{i0}, V_{j0}, \delta_{i0}, \delta_{j0})$$

$$h_m = h_{m0} + K_1(V_i - 1) + K_2(V_j - 1) + K_3(\delta_i) + K_4(\delta_j)$$

Where,

$$K_1 = \frac{\partial h}{\partial V_i}\Big|_{m=m_0}$$

$$K_2 = \frac{\partial h}{\partial V_j}\Big|_{m=m_0}$$

$$K_3 = \frac{\partial h}{\partial \delta_i}\Big|_{m=m_0}$$

$$K_4 = \frac{\partial h}{\partial \delta_j}\Big|_{m=m_0}$$

By employing this methodology, the equations f_{1i}, f_{2i}, g_{1i} and g_{2i} are linearised,

$$F_{ijA}(t) = \cos(\theta_{ij}) + \cos(\theta_{ij}) \cdot (V_i(t) - 1) + \cos(\theta_{ij}) \cdot (V_j(t) - 1) - \sin(\theta_{ij}) \cdot \delta_j(t) \quad (32)$$

$$F_{ijB}(t) = \sin(\theta_{ij}) \cdot \delta_i(t) \quad (33)$$

$$G_{ijA}(t) = \cos(\theta_{ij}) \cdot \delta_i(t) \quad (34)$$

$$G_{ijB}(t) = -[\sin(\theta_{ij}) + \sin(\theta_{ij}) \cdot (V_i(t) - 1) + \sin(\theta_{ij}) \cdot (V_j(t) - 1) + \cos(\theta_{ij}) \cdot \delta_j(t)] \quad (35)$$

The linearised power flow equations is composed by the linear equations above,

$$P_i(t) = \sum_{j=1}^{N} Y_{ij}[F_{ijA}(t) + F_{ijB}(t)] \quad (36)$$

$$Q_i(t) = \sum_{j=1}^{N} Y_{ij}[G_{ijA}(t) + G_{ijB}(t)] \quad (37)$$

And when expanded, the linearised form of the power flow equations are obtained.

$$P_i(t) = \sum_{j=1}^{N} Y_{ij}[\cos(\theta_{ij}) + \cos(\theta_{ij}) \cdot (V_i(t) - 1) + \cos(\theta_{ij}) \cdot (V_j(t) - 1) - \sin(\theta_{ij}) \cdot \delta_j(t) + \sin(\theta_{ij}) \cdot \delta_i(t)] \quad (38)$$

$$Q_i(t) = \sum_{j=1}^{N} Y_{ij}[\cos(\theta_{ij}) \cdot \delta_i(t) - \cos(\theta_{ij}) \cdot \delta_j(t) - \sin(\theta_{ij}) - \sin(\theta_{ij}) \cdot (V_i(t) - 1) - \sin(\theta_{ij}) \cdot (V_j(t) - 1)] \quad (39)$$

H. Objective Function

Following the objectives of distribution grid voltage control, the main objective function of the problem is to reduce the voltage deviation from the operating point 1 p.u. This operating point has been chosen to fulfil the requirements of a distribution grid: keep the voltage level in acceptable range at the consumer terminals, increase the stability margin and protect the equipment from voltage deviations over long periods of time. Therefore, reducing the voltage deviations is the main focus of this paper.

The degrees of freedom of the problem are defined by all decision variables and state variables (which depend on the decision variables). They are represented with the vectors **u** and **x** respectively.

$$\mathbf{u} = (P_1, Q_1, P^G_{n_B}, Q^G_{n_B}, Q^G_{n_{pv}})$$

$$\mathbf{x} = (V_{i:i\in Set_{bus}}, \delta_{i:i\in Set_{bus}}, P_{i:i\in[2...N]}, Q_{i:i\in[2...N]})$$

These vectors have values for every time step $t \in [1...T]$, but they are displayed as scalar variables for clarity's sake.

To improve voltage control, a decision variable which is the voltage deviation from the operation point is set in the objective function. Thus, the optimisation problem tries to minimise the voltage deviation from the operating voltage for all buses and time periods.

$$\min_{\mathbf{u},\mathbf{x}} \sum_{t=1}^{T}\sum_{i=1}^{N}|V_i(t) - 1| \tag{40}$$

However, the solver used for the simulation has troubles to handle absolute values. $v_{dev,i}$ is declared and it has to fulfil the constraint equations (42) which is a linear expression for absolute voltage deviation from operation point:

$$\min_{\mathbf{u},\mathbf{x}} \sum_{t=1}^{T}\sum_{i=1}^{N} v_{dev,i}(t) \tag{41}$$

$$v_{dev,i}(t) \geq V_i(t) - 1,\ v_{dev,i}(t) \geq 1 - V_i(t),\ v_{dev,i}(t) \geq 0 \tag{42}$$

With the aforementioned formulation, the variable $v_{dev,i}$ represents the absolute deviation from the operation point (hence the positive value) employing exclusively linear constraints.

III. Demo-Case Description

A. Topology of the Distribution Grid

In the real demo-case grid there are two LV networks connected to the PV substation and the battery substation respectively. The PV substation is at the same time composed by two transformers connected to two groups of loads with different nominal voltages: $400V$ (stadium loads) and $240V$ (industrial and household clients). Since the Skagerak EnergiLAB is not yet completed, the current topology is missing the PV and battery connections, which is estimated based on the information provided by Skagerak Nett.

1) Loads: The loads are shown in Figure 1 as black arrows, located at the end of the branches. They correspond to different customers. On each node there might be from 1 to several aggregated clients. They correspond to commercial and residential consumption points. One of the most important things to note are the floodlights located on node $B2$. Another large load is the one located in the nodes $S2$. On the $240V$ side, there is one large load, which is $H12$. The loads at the nodes $S4$, $S5$, $H4$, $H6$, $B3$ are noticeable but lower than those mentioned previously. The loads located at $S6$, $H8$, $H9$, $H10$ are considerably smaller and lack load measurements, therefore they are estimated based on yearly values.

2) PV generation: The PV system consists of three separated main modules, one on each roof of the stadium (beside the north roof area). These three groups contain several inverters each. In order to model them, four nodes are added into the topology: $PV1$, $PV2$, $PV3$ and $PV4$. $PV1$ is connected to $S1$ and has a module connected to, which represents 38.5% of the total power generated on all modules. $S1$ is also connected to $PV2$, which is a link for the other two PV modules, located in nodes $PV3$ and $PV4$, which represent 23% and 38.5% of the total power respectively. Even though there are more than three PV inverters, three "aggregated" inverters are assumed, which will represent the total active and reactive power of the three PV modules.

Other important properties of the PV system are:

- Total installed power: $690kWp$
- Total inverter capacity: $750kVA$

B. Battery Characteristics

The battery is a Lithium-ion type connected through an inverter under the transformer in the battery substation. Through a cable it is linked to the bar $B1$ as another load/generator, in a new node $B4$.

The operation properties of the battery are described below:

- Total battery capacity: $1MWh$.
- Maximum charge and discharge power: $\pm 333.3kW$ (the battery can be charged and discharged in three hours, which is the recommended battery capacity when the stadium is connected to the grid, compared to the maximum $1MW$ capacity for off-grid mode).
- Charge/discharge efficiency: 0.95.
- Inverter capacity: 2.5% larger than the maximum charge-discharge power (in order to be capable of using reactive power at any operation point).

C. Total System

Once the grid has been completely defined and modelled, the simulation can be performed. It consists on 30 nodes, it has a battery and 3 PV modules with an inverter each. The total topology can be seen in Figure 1. The battery and PV modules will not be directly connected in the real grid due to practical issues. However, as a part of the study it is very relevant to include the battery and floodlight loads in the stadium grid, to

study the whole system as a smart grid. Thus, for the system analysis the battery substation does not provide any energy, and the two grids are connected through a line going from $B1$ to $S1$.

Then, the formulation of the problem is applied on the demo-case. The PV equations are updated with the three PV modules. n_{PV} is the set of PV nodes, which is $n_{PV} \in [PV1, PV3, PV4]$. The modelling of the PV system is divided into two groups depending on the forecast horizon. A first short term deterministic forecast that covers h hours is applied. Then, the PV is modelled for the rest of the horizon (from h to T) employing a chance-constraint of the active power. That is defined with a given monthly maximum and minimum quantiles of historic PV production, π_P (for example, the lowest boundary could be the quantile 0.01 and the highest 0.99, in order to include all possible outcomes of PV production). To obtain historical PV production on the site, the only available data are radiation (in kW/m^2) because the PV installation is very recent. Then, the power is obtained from the system's PV surface, solar radiation and characteristics of the module and environment using a linear method based on the one used in [36].

$$P_{PV} = c_F \cdot \eta_{PV} \cdot \eta_{bos} \cdot S_{PV} \cdot p_{rad} \tag{43}$$

where P_{PV} is the power generated by the PV system in kW, p_{rad} is the horizontal radiation on the surface in kW/m^2. That is assuming flat PV modules on the surface. S_{PV} is the PV surface in m^2 ($5330m^2$ for the demo-case divided in three PV groups: 38.5% of the surface is in $PV1$, 23% in $PV3$ and 38.5 in $PV4$), $\eta_{PV} = 0.158$ is the conversion efficiency of the PV modules, $\eta_{bos} = 0.91$ is the system efficiency. In order to correct the equation to take into account unavoidable shadowing, the modules' tilt angle, orientation angle etc. a correction factor c_F (in this case taken as 0.95) is added to the equation. Thus, the total PV equations are:

$$\hat{P}^G_{n_{PV}}(t) = P_{n_{PV}}(t) + P^L_{n_{PV}}(t) \quad \forall t \in [t, t+1, ..., t+h] \tag{44}$$

$$\begin{aligned} &\underline{P}^G_{n_{PV},\pi_P}(t) \leq P_{n_{PV}}(t) + P^L_{n_{PV}}(t) \leq \overline{P}^G_{n_{PV},\pi_P}(t) \\ &\forall t \in [t+h+1, ..., T] \end{aligned} \tag{45}$$

$$S^2_{inv,R16}(t) \geq (\hat{P}^G_{n_{PV}})^2(t) + (Q^G_{n_{PV}})^2(t) \quad \forall t \in [t, t+1, ..., t+h] \tag{46}$$

$$\begin{aligned} &S^2_{inv,n_{PV}}(t) \geq (\underline{P}^G_{n_{PV},\pi_P})^2(t) + (Q^G_{n_{PV}})^2(t) \\ &\forall t \in [t+h+1, ..., T] \end{aligned} \tag{47}$$

For all the simulations of this paper, different quantiles ranges of historic PV production were tested. The conclusion out of the results is that they do not influence on the most recent results (with 1h ahead forecasts) since the short time forecast is deterministic and updated every hour. Therefore, the system is optimised for every time period without much influence of the previous simulations (where historical PV quantile range is considered). Thus, the results are shown for the last updated time-steps ($1h$ SARIMA forecasts) in this paper. Nonetheless, the tool is capable to be developed further to carry scheduling problems where both long and short term forecasts are equally important, in the cases where deviations from the $24h$ scheduling may derive to economic penalisations. The short term updated $1h$ forecasts are monthly SARIMA models (created with the Python library [37]), which consists of two models each month combined, with coefficients $(1, 1, 1)$ for the ARIMA part and $(1, 1, 1, 24)$ for the seasonal part (the seasonal term 24 refers to a $24h$ seasonality of the data, which characterises PV production). These coefficients provided the lowest error and fastest calculations with the available data. The battery node is $n_B = B4$. It is also of interest to analyse the costs of the purchased energy in order to analyse other battery services together with voltage control. For that purpose, a multi-objective function is used. Historical day-ahead electricity prices are used for the analysed distribution grids, located in the zone of Kristiansand (southern Norway). The data located on the nordpool website[5] can be obtained with hourly resolution from the year 2013 up to today. The new problem formulation is then presented below:

$$\min_{\mathbf{u},\mathbf{x}} \; a \sum_{t=1}^{T} \sum_{i=1}^{N} v_{dev,i}(t) + b \sum_{t=1}^{T} C_{import}(t) \cdot P_{import}(t) \cdot \Delta t$$

s.t.

eqs. (1) to (9), (12) to (25), (28), (38), (39) and (44) to (47) (48)

Here, a and b represent weighting parameters that evaluate the case where voltage deviation or energy costs have more importance respectively. In the next section the optimisation problem is inserted into the receding horizon algorithm. After that, in Section V the operation of the system with different weighting of the two objective function terms, voltage deviation on the whole system and energy price C_{import} are analysed.

IV. Receding horizon algorithm

The receding horizon algorithm is presented in algorithm 1. n_{days} is in this case set to 7 and t_s (the horizon expansion period) is 12 hours assuming that the new prices are known at noon for the next day. H_d is the day's length, that means 24 time-periods, or 24 hours. For every day the receding horizon is applied. There are three types of situations. The first day, the control is applied from the beginning of the first day until the receding expansion period t_{rec}. The second case applies to all days except first and last. In this second case, the receding horizon loop is applied from t_{rec} to the next expansion of the horizon (in total 24 hours). The third type of situation occurs during the last day. There is no more horizon expansion and therefore, the end period of the receding horizon is at the end of the last day $t_{hn_{days}}$.

[5] https://www.nordpoolgroup.com/

n_{days}, t_s, t_1, H_d;
for *day = 0...*n_{days} **do**
  if $day = n_{days}$ *(last day)* **then**
    Last simulation period is the last period of the day: $T = t_{hn_{days}}$;
    The receding horizon is calculated until the end of the day: $t_{rec} = t_{hn_{days}}$;
  if $day = 0$ *(first day)* **then**
    $t_{period} = t_1$;
    $T = t_{period} + H_d - 1$;
    $t_{rec} = t_{period} + t_s$;
  else
    In the case of a day different from the first $T = t_{period} + (H_d - 1) + (H_d - t_s)$;
    $t_{rec} = t_{period} + H_d$;
  end
  for $t = t_{period}...t_{rec}$ **do**
    Solve optimisation problem 48 for the time vector $[t...T]$;
    Save state of charge of the battery $SoC(t)$;
    $t_{period} = t + 1$, update the value of t_{period};
  end
end

Algorithm 1: Pseudo code for a complete simulation with receding horizon for the demo-case Skagerak EnergiLab.

V. Results

In this section the results of the simulations are presented. The operation and different use cases of the battery are shown in the nodes of the system where the loads are larger. That means that the risk for unacceptable voltage deviation is higher, namely in node $B2$, where the floodlights of the stadium are located. Also in node $B4$, where the battery is connected.

The simulations were carried in four weeks of the year, 26th November-2nd December 2017, 23-29th April 2018, 8-14th July 2018 and 6-12th August 2018 and the quantitative analyses are shown in Tables I and II. Four different cases are analysed. Case I considers no battery installed and no reactive power use from PV and battery inverters. Case II considers the installation of the battery and prioritises lower energy costs ($a = b = 1$), but no reactive power is used. Case III is the same as Case II but including reactive power. Finally, Case IV is similar to Case III but changing the weighting of the objective function to prioritise voltage deviation ($a = 100$, $b = 0.01$).

In Figure 2 the operation of the studied battery is shown. These results are shown for Case III with comparisons to Case I (in Figure 2a) and to Cases I and II (in Figure 2d). It is observed that under this configuration, the most optimal solution seeks to charge the battery when the energy price is lower and discharge when it increases, in order to decrease energy import from the grid when prices are high (Figure 2a-b). However, reactive power by the battery inverter is also used to reduce voltage deviation in the system (Figure 2b-c), despite of extra voltage peaks caused by the sudden charge and discharge of the battery.

Figure 3 shows the effect of different weighting of the objective function. Since it is difficult to compare both terms (they do not have the same units), two extreme values are analysed. Case I-III gives most of the priority to lower energy costs and Case IV to prioritise lower voltage deviation. In Figure 3a and b one can see that if voltage deviation is preferred, the voltage peak is reduced compared to the other case (Figure 3b). This is achieved by charging the battery during the morning from energy from the grid (Figure 3a) and use this charged energy during the floodlight use, as seen in Figure 3c. This shows a coordination of active and reactive power use to control voltage deviations locally. This can be especially seen in Figure 3c, where the battery is discharged during the use of the floodlights (8th of July, $4 - 6$ p.m.) in order to reduce the voltage peak. It is important to remark that the studied network is very robust and voltage peaks are always below unacceptable levels (a maximum voltage deviations assumed as acceptable at the demo-case will be $\pm 5\%$, following [38]).

It is observed that depending on the balance in the objective function it can affect both voltage deviation and energy costs. When voltage deviation is prioritised and reactive power is used, the voltage deviations can be reduced up to 72% (Case IV) compared to Case I, with no use of battery. This is caused due to the use of active power to reduce voltage peaks, as well as a smoother charge and discharge of the battery to avoid extra voltage peaks. However, the energy costs are higher in this case compared to Case I, considering the results of Table II. Nonetheless, when a lower energy cost is preferred then, the voltage deviations are larger (but still lower than without battery thanks to reactive power use, as in Case III) and the energy cost is slightly lower in comparison with the base case with no battery (up to a 2.76% in November). The small reduction in price is explained by the flat prices of electricity in Norway, with a maximum standard deviation of $12.4€/MWh$ in the week of November, which presents the large price peaks (and therefore higher savings using the battery in Cases II and III). In the other weeks this value varies from $2.24€/MWh$ and $3.94€/MWh$. In other cases with more fluctuating prices the savings can be more significant.

VI. Conclusions and future work

As seen in the simulations, the battery can offer an improved voltage regulation by using reactive control (provided by the inverter) and using its capacity to charge and discharge at specific times to affect the voltage levels. This has been described in Section V, where a combination of active and reactive control can reduce the system's voltage deviation from 34% to 72%, depending on the priorities (energy arbitrage or voltage control). One of the costs of the improved voltage regulation is that the battery is limited to provide certain services like energy arbitrage when voltage regulation is prioritised. That

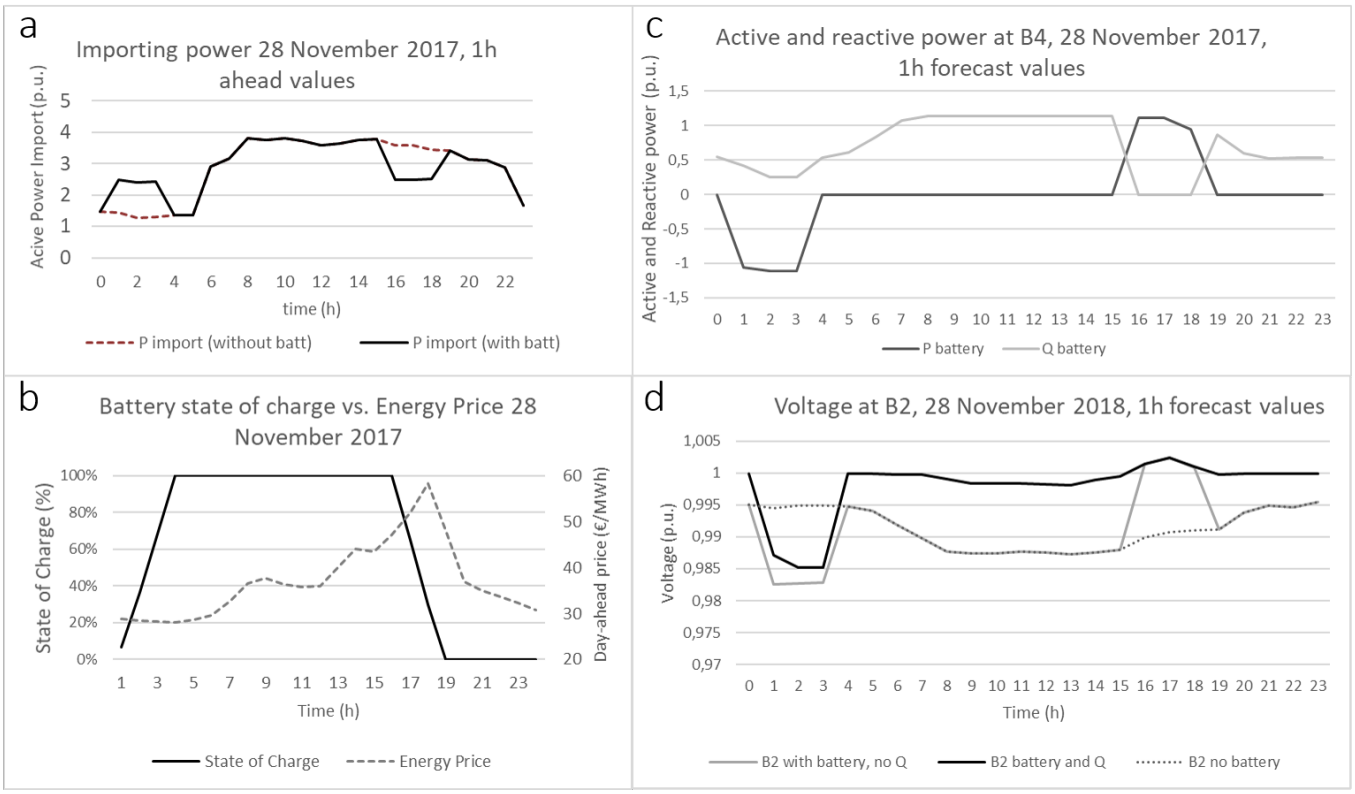

Fig. 2. Results of one day of operation, the 28th of November with 1h forecast values and weighting towards lower cost. Figure 2a represents the importing power from the grid for Case III and Case I. One can appreciate the load shifting in Case III, from $4-6$ p.m. to $1-3$ a.m, where energy is cheaper. This can be appreciated in Figure 2b, where the battery is charged when prices are low and discharged when they are high, causing this energy shift in Figure 2a (reducing the energy costs in 2.8% or 22€ for that day). In Figure 2c, the active and reactive power at battery node ($B2$) is represented for Case III. It is observed that the inverter uses positive reactive power (a total of $5.01Mvar$) in Case III to compensate the voltage drop in the line (achieving a 71.1% reduction in the voltage deviation for that day compared to Case I and 72.7% compared to Case II). Nevertheless, the use of reactive power decreases when active power is used to charge and discharge the battery, since it has to fulfil the inverter equation (24). In Figure 2d, the voltage at the node $B2$ is represented, which is the node with highest voltage drops due to the stadium floodlights. It is seen that the use of reactive power reduces considerably the voltage peak, but the battery causes at the same time extra voltage peaks when charging and discharging.

TABLE I
SUM OF ALL VOLTAGE DEVIATIONS AND CHANGE COMPARED TO CASE I (%)

$\sum v_{dev}(p.u.)$	Case I	Case II	Case III	Case IV
November	11.24	12.70	7.41	4.54
April	27.39	28.89	17.55	15.47
July	15.84	16.57	6.33	5.53
August	12.84	14,14	6.29	3.60
change (%)	Case I	Case II	Case III	Case IV
November	0.0	13.0	-34.0	-59.6
April	0.0	5.5	-35.9	-43.5
July	0.0	4.6	-60.0	-65.1
August	0.0	10.1	-51.0	-72.0

TABLE II
ENERGY COSTS (€/WEEK) AND CHANGE COMPARED TO CASE I (%)

E. Costs (€)	Case I	Case II	Case III	Case IV
November	5,723.67	5,565.94	5,565.94	5,744.54
April	2,176.54	2,141.71	2,141.71	2,205.33
July	4,414.42	4,405.22	4,405.22	4,462.93
August	4,416.92	4,386.52	4,386.52	4,443.63
Change (%)	Case I	Case II	Case III	Case IV
November	0.00	-2.76	-2.76	0.36
April	0.00	-1.60	-1.60	1.32
July	0.00	-0.21	-0.21	1.10
August	0.00	-0.69	-0.69	0.60

is caused by the relationship between fast charge and discharge with voltage peaks.

The installation of a battery can bring multiple benefits to a LV distribution network. It can be used for energy arbitrage and load shifting, as seen in the previous section (with the corresponding price reduction of up to 2.72%). Other services such as peak shaving could also be provided. Additionally, the battery can contribute to the grid stability by employing reactive power provided by its inverter to reduce the large voltage deviations. The same services can be provided by photovoltaic systems, reducing peaks greatly and thus avoiding active power curtailment. The battery can also provide voltage regulation by using its active power and capacity, which means using its stored energy to supply a nearby high

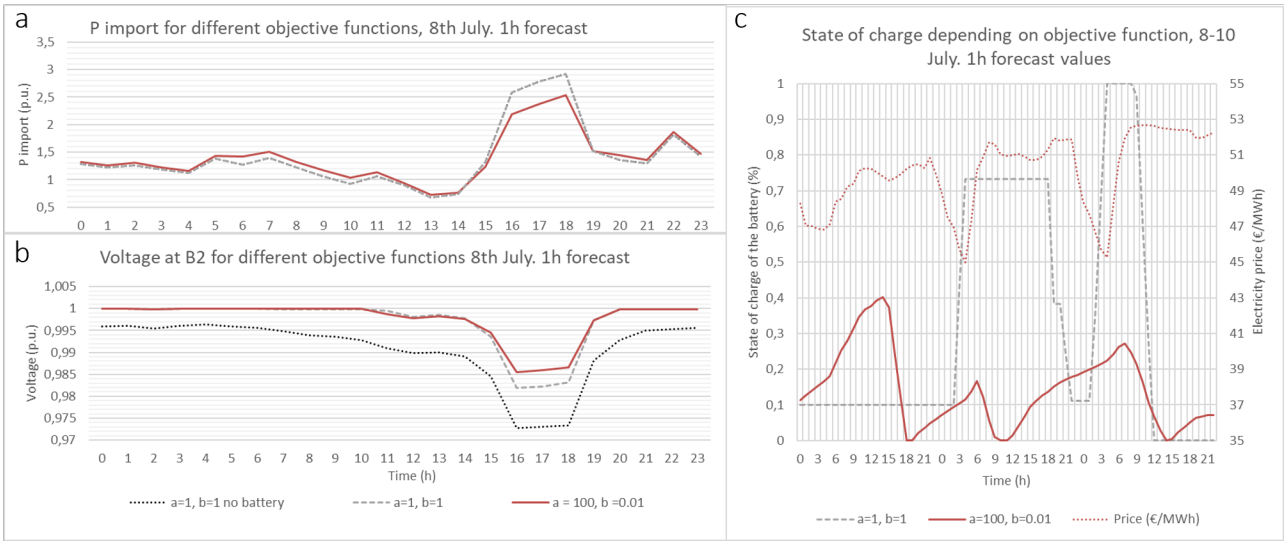

Fig. 3. Different priorities in the cost function, from more weighting of the energy costs ($a = 1$, $b = 1$, Case III) to more priority of voltage deviations ($a = 100$, $b = 0.01$, Case IV). In Figure 3a, the power import from the grid (at node 1) on the 8th of July 2018 is shown. In Figure 3b, the voltage profile of the node where the floodlights are located ($B2$) can be seen. The different charging strategies of the battery are displayed in Figure 3c for the days 8-10th of July 2018.

load (peak), buffering slightly the voltage peak. However, the opposite trends of the weighting terms of the objective function indicate the need for a way to quantify both terms of the cost function in €, by for example modelling the local market, and considering the investment and operational costs of the battery. Then, an optimal solution with the lowest overall costs could be achieved.

The battery can also help integrating PV systems into the grid by storing energy that is not needed at the generation time. However, in the studied demo-case the loads where high and PV produced power was always consumed. Due to the linearisation of the power flow equations employed in this paper, the possibility of analysing network losses was not possible, but it can be implemented in the future. Regarding investment deferral, the studied demo-case network is currently very strong. Most of the cables are largely under capacity limits, and for example the cable connecting to the floodlights has a maximum peak of 47.2% in the week with the highest load. During other time steps the used capacity is much lower. That means it is difficult to prove that the battery can be used to defer grid investment upgrades, but with the methods developed in this paper it would be possible to test in other networks, comparing the battery costs with the installation of new lines.

Another outcome of this study is the Python tool. It will be further developed as part of the IPN project IntegER, in order to assess future studies. The flexibility of its structure facilitate the creation and modification of new data modules, the use of different solvers depending on the available licences, etc.

There are several research aspects presented in this paper that may be continued forward. The model and Python tool are flexible enough to be used in future challenges. Here are some of the aspects that can be further discussed without giving them any particular preference:

- The linearisation of the power flow equations can be improved by adding power losses and improving the accuracy. That would allow answering more research questions about battery use.
- The analysis of different grid topologies and different loads can be useful to provide a more complete study of the battery uses in a LV network.
- Since batteries suffer from ageing and degradation, it is reasonable to study these phenomena on the battery, and suggest operation guidelines and economic consequences.
- The estimation of PV generation can be improved applying diffusive radiation to obtain a more precise power calculation.
- Even though the system is optimised, the real PV production and the real time response of the system to unexpected PV change needs to be further explored. So far, 1h forecasts are considered to be the same as the real production.
- More exact short-term forecasts can be explored, considering exogenous values like cloud coverage. The lack of this data during the paper period did not allow the improvement of these models.
- Other alternatives for 24h PV forecasts can be tested to improve the current problem formulation. Some examples include stochastic methods such as scenarios or 24h forecasts with or without include weather information depending on the availability of it.
- Other economical markets and frameworks (different util-

ity tariffs, other countries, etc.) can be tested in order to analyse the benefits of installing a battery (energy arbitrage, peak shaving, load shifting, PV integration).
- The possibility of coordination between the different voltage control elements to provide a more stable voltage profile in the whole system could be investigated as well.
- Make a purely economic analysis (including investment and operation) where the battery is used to obtain the maximum economic benefit and thus, voltage control is used to keep the voltage within acceptable limits.

REFERENCES

[1] O. Ellabban, H. Abu-Rub, and F. Blaabjerg, "Renewable energy resources: Current status, future prospects and their enabling technology," *Renewable and Sustainable Energy Reviews*, vol. 39, pp. 748–764, 2014.

[2] J. Schmid, A. Hauer, D. Schmidt, M. Schmidt, F. Staiß, G. Stadermann, M. Sterner, and G. Stryi-Hipp, "Energiekonzept 2050: Eine Vision für ein nachhaltiges Energiekonzept auf Basis von Energieeffizienz und 100% erneuerbaren Energien, Forschungsverbund Erneuerbare Energien (fvee), Berlin, 2010."

[3] J. P. Lopes, N. Hatziargyriou, J. Mutale, P. Djapic, and N. Jenkins, "Integrating distributed generation into electric power systems: A review of drivers, challenges and opportunities," *Electric power systems research*, vol. 77, no. 9, pp. 1189–1203, 2007.

[4] F. P. Sioshansi, *Smart grid: integrating renewable, distributed and efficient energy*. Academic Press, 2011.

[5] R. R. Appino, J. Á. G. Ordiano, R. Mikut, T. Faulwasser, and V. Hagenmeyer, "On the use of probabilistic forecasts in scheduling of renewable energy sources coupled to storages," *Applied Energy*, vol. 210, pp. 1207–1218, 2018.

[6] R. R. Appino, M. Muñoz Ortiz, J. A. G. Ordiano, R. Mikut, V. Hagenmeyer, and T. Faulwasser, "Reliable dispatch of renewable generation via charging of time-varying PEV populations," *IEEE Transactions on Power Systems*, vol. 34, pp. 1558–1568, 2019.

[7] S. Frank and S. Rebennack, "An introduction to optimal power flow: Theory, formulation, and examples," *IIE Transactions*, vol. 48, no. 12, pp. 1172–1197, 2016.

[8] G. Poursharif, A. Brint, M. Black, and M. Marshall, "Analysing the ability of smart meter data to provide accurate information to the UK DNOs," *CIRED-Open Access Proceedings Journal*, vol. 2017, no. 1, pp. 2078–2081, 2017.

[9] N. Leemput, F. Geth, B. Claessens, J. Van Roy, R. Ponnette, and J. Driesen, "A case study of coordinated electric vehicle charging for peak shaving on a low voltage grid," in *3rd IEEE PES International Conference and Exhibition on Innovative Smart Grid Technologies (ISGT Europe)*. IEEE, 2012, pp. 1–7.

[10] V. Annathurai, C. Gan, M. Ghani, and K. Bahrain, "Necessity of time-series simulation for the investigation of high penetration of photovoltaic systems in Malaysia," *Journal of Telecommunication, Electronic and Computer Engineering (JTEC)*, vol. 10, no. 2-2, pp. 57–61, 2018.

[11] N. Mithulananthan, D. Q. Hung, and K. Y. Lee, *Intelligent network integration of distributed renewable generation*. Springer, 2016.

[12] M. N. Kabir and Y. Mishra, "Utilizing reactive capability of PV inverters and battery systems to improve voltage profile of a residential distribution feeder," in *PES General Meeting— Conference & Exposition, 2014 IEEE*. IEEE, 2014, pp. 1–5.

[13] E. Dall'Anese, K. Baker, and T. Summers, "Chance-constrained AC optimal power flow for distribution systems with renewables," *IEEE Transactions on Power Systems*, vol. 32, no. 5, pp. 3427–3438, 2017.

[14] M. Koller, T. Borsche, A. Ulbig, and G. Andersson, "Review of grid applications with the Zurich 1 MW battery energy storage system," *Electric Power Systems Research*, vol. 120, pp. 128–135, 2015.

[15] B. Faessler, M. Schuler, M. Preißinger, and P. Kepplinger, "Battery storage systems as grid-balancing measure in low-voltage distribution grids with distributed generation," *Energies*, vol. 10, no. 12, p. 2161, 2017.

[16] G. Hilton, A. Cruden, and J. Kent, "Comparative analysis of domestic and feeder connected batteries for low voltage networks with high photovoltaic penetration," *Journal of Energy Storage*, vol. 13, pp. 334–343, 2017.

[17] T. Ku, C. Lin, C. Chen, and C. Hsu, "Coordination of transformer on-load tap changer and PV smart inverters for voltage control of distribution feeders," in *Industrial and Commercial Power Systems Technical Conference (I&CPS), 2018 IEEE/IAS 54th*. IEEE, 2018, pp. 1–8.

[18] G. Fitzgerald, J. Mandel, J. Morris, and H. Touati, "The economics of battery energy storage: How multi-use, customer-sited batteries deliver the most services and value to customers and the grid," *Rocky Mountain Institute*, 2015.

[19] H. C. Hesse, M. Schimpe, D. Kucevic, and A. Jossen, "Lithium-ion battery storage for the grid - a review of stationary battery storage system design tailored for applications in modern power grids," *Energies*, vol. 10, no. 12, p. 2107, 2017.

[20] M. Müller, L. Viernstein, C. N. Truong, A. Eiting, H. C. Hesse, R. Witzmann, and A. Jossen, "Evaluation of grid-level adaptability for stationary battery energy storage system applications in europe," *Journal of Energy Storage*, vol. 9, pp. 1–11, 2017.

[21] Y. Yang, H. Li, A. Aichhorn, J. Zheng, and M. Greenleaf, "Sizing strategy of distributed battery storage system with high penetration of photovoltaic for voltage regulation and peak load shaving," *IEEE Transactions on Smart Grid*, vol. 5, no. 2, pp. 982–991, 2014.

[22] E. L. Ratnam and S. R. Weller, "Receding horizon optimization-based approaches to managing supply voltages and power flows in a distribution grid with battery storage co-located with solar PV," *Applied Energy*, vol. 210, pp. 1017–1026, 2018.

[23] K. Schneider, B. Mather, B. C. Pal, C.-W. Ten, G. Shirek, H. Zhu, J. Fuller, J. L. R. Pereira, L. Ochoa, L. De Araujo *et al.*, "Analytic considerations and design basis for the IEEE distribution test feeders," *IEEE Transactions on Power Systems*, vol. 33, no. 3, pp. 3181–3188, 2018.

[24] "Benchmark systems for network integration of renewable and distributed energy resources," Cigre Task Force C6.04.02, Tech. Rep., 2014. [Online]. Available: http://c6.cigre.org/Publications/Technical-Brochures

[25] P. Fortenbacher, M. Zellner, and G. Andersson, "Optimal sizing and placement of distributed storage in low voltage networks," in *Power Systems Computation Conference (PSCC), 2016*. IEEE, 2016, pp. 1–7.

[26] P. Fortenbacher, "On the integration of distributed battery storage in low voltage grids," Ph.D. dissertation, ETH Zurich, 2017.

[27] P. Fortenbacher and T. Demiray, "Linear/quadratic programming based optimal power flow using linear power flow and absolute loss approximations," *arXiv preprint arXiv:1711.00317*, 2017.

[28] D. Zarrilli, A. Giannitrapani, S. Paoletti, and A. Vicino, "Receding horizon voltage control in LV networks with energy storage," in *55th Conference on Decision and Control (CDC)*. IEEE, 2016, pp. 7496–7501.

[29] J. von Appen, T. Stetz, M. Braun, and A. Schmiegel, "Local voltage control strategies for PV storage systems in distribution grids," *IEEE Transactions on Smart Grid*, vol. 5, no. 2, pp. 1002–1009, 2014.

[30] M. Muñoz Ortiz, "Voltage control in smart distribution systems: the value of battery flexibility," Master's thesis, Karlsruhe Institute of Technology, 2018.

[31] R. D. Zimmerman, C. E. Murillo-Sánchez, R. J. Thomas *et al.*, "Matpower: Steady-state operations, planning, and analysis tools for power systems research and education," *IEEE Transactions on power systems*, vol. 26, no. 1, pp. 12–19, 2011.

[32] T. Brown, J. Hörsch, and D. Schlachtberger, "Pypsa: Python for power system analysis," *arXiv preprint arXiv:1707.09913*, 2017.

[33] W. E. Hart, J.-P. Watson, and D. L. Woodruff, "Pyomo: modeling and solving mathematical programs in Python," *Mathematical Programming Computation*, vol. 3, no. 3, pp. 219–260, 2011.

[34] Y. Levron, J. M. Guerrero, and Y. Beck, "Optimal power flow in microgrids with energy storage," *IEEE Transactions on Power Systems*, vol. 28, no. 3, pp. 3226–3234, 2013.

[35] T. Akbari and M. T. Bina, "A linearized formulation of ac multi-year transmission expansion planning: A mixed-integer linear programming approach," *Electric Power Systems Research*, vol. 114, pp. 93–100, 2014.

[36] J. G. d. S. F. Junior, T. Oozeki, H. Ohtake, T. Takashima, and O. Kazuhiko, "On the use of maximum likelihood and input data

similarity to obtain prediction intervals for forecasts of photovoltaic power generation," *Journal of Electrical Engineering & Technology*, vol. 10, no. 3, pp. 1342–1348, 2015.

[37] S. Seabold and J. Perktold, "Statsmodels: econometric and statistical modeling with Python," in *Proceedings of the 9th Python in Science Conference*, vol. 57. SciPy society Austin, 2010, p. 61.

[38] M. Bollen, Y. Beyer, E. Styvactakis, J. Trhulj, R. Vailati, and W. Friedl, "A European benchmarking of voltage quality regulation," in *15th IEEE International Conference on Harmonics and Quality of Power (ICHQP)*. IEEE, 2012, pp. 45–52.